Sorting of Membrane Components from Endosomes and Subsequent Recycling to the Cell Surface Occurs by a Bulk Flow Process

Satyajit Mayor, John F. Presley, and Frederick R. Maxfield

Columbia University, College of Physicians and Surgeons, New York

Abstract. A central question in the endocytic process concerns the mechanism for sorting of recycling components (such as transferrin or low density lipoprotein receptors) from lysosomally directed components; membrane-associated molecules including receptors are generally directed towards the recycling pathway while the luminal content of sorting endosomes, consisting of the acid-released ligands, are lysosomally targeted. However, it is not known whether recycling membrane receptors follow bulk membrane flow or if these proteins are actively sorted from lysosomally directed material because of specific protein sequences and/or structural features. Using quantitative fluorescence microscopy we have determined the endocytic route and kinetics of traffic of the bulk carrier, membrane lipids, to address this issue directly. We show that *N*-[*N*-(7-nitro-2,1,3-benzoxadiazol-4-yl)-ε-aminohexanoyl]-sphingosylphosphorylcholine (C_6-NBD-SM) in endocytosed as bulk membrane, and it transits the endocytic system kinetically and morphologically identically to fluorescently labeled transferrin in a CHO cell line. With indistinguishable kinetics, the two labeled markers sort from lysosomally destined molecules in peripherally located sorting endosomes, accumulate in a peri-centriolar recycling compartment, and finally exit the cell. Other fluorescently labeled lipids, C_6-NBD-phosphatidylcholine and galactosylceramide also traverse the same pathway. The constitutive nature of sorting of bulk membrane towards the recycling pathway and the lysosomal direction of fluid phase implies a geometric basis of sorting.

INTRACELLULAR trafficking of proteins during endocytosis has been extensively characterized (see Fig. 1). This process is mediated by organelles such as coated vesicles, sorting endosomes or early endosomes, and late endosomes (Goldstein et al., 1985; Maxfield and Yamashiro, 1991; van Deurs et al., 1989). A central question in the endocytic process concerns the mechanism for sorting of recycling components (e.g., the transferrin receptor [Tf-R][1] or the low density lipoprotein receptor [LDL-R]) from lysosomally directed components (e.g., acid-released ligands such as low density lipoprotein [LDL] or α_2-macroglobulin [α_2-M]). This sorting is a rapid step ($t_{1/2} < 3$ min), and as depicted in Fig. 1, takes place in acidic organelles called sorting endosomes (Yamashiro and Maxfield, 1987), having a tubular-vesicular morphology (Geuze et al., 1983; Gruenberg et al., 1989; Mellman et al., 1986). This is also where acid-released ligands accumulate and are eventually delivered to lysosomes via a maturation process (Dunn and Maxfield, 1992; Stoorvogel et al., 1991). The rate of sorting is thus related to the rate of removal of the recycling components from the sorting endosome.

Once removed from the sorting endosome, recycling components are delivered to a separate recycling compartment, morphologically and functionally distinct from sorting endosomes (Maxfield and Yamashiro, 1991). This compartment, in CHO cells, is a collection of tubular endosomes concentrated in the peri-centriolar region of the cell, containing recycling receptors, such as Tf-R and LDL-R but not lysosomally directed ligands such as LDL or α_2-M (McGraw et al., 1993; Yamashiro et al., 1984). The recycling compartment has also been recently characterized as a tubular network located around the peri-centriolar region in AtT20, HeLa, and other cells (Tooze and Hollinshead, 1991).

A striking feature of the endocytic system is the high efficiency of recycling of membrane receptors and the lysosomal direction of their acid-released ligands, albeit at lower efficiency (for review see van Deurs et al., 1989). There are two ways by which this process may take place: (1) by a selective process in which recycling molecules are specifically removed from the sorting endosome while lyso-

1. *Abbreviations used in this paper*: α_2M, α_2-macroglobulin; C_6-NBD-PC, C_6-NBD-phosphatidylcholine; C_6-NBD-SM, *N*-[*N*-(7-nitro-2,1,3-benzoxadiazol-4-yl)-ε-aminohexanoyl]-sphingosylphosphorylcholine; CCD, charged-couped device; Cy3-α_2M, Cy3-labeled α_2M; DiO-LDL, 3,3'dioctadecyloxacarbocyanine-labeled LDL; DiI-LDL, 3,3'-dioctadecylindocarbocyanine-labeled LDL; HF-12, Hepes-buffered Hams F-12 medium; LDL, low density lipoprotein; LDL-R, LDL-receptor; Rh-Tf, rhodamine-labeled Tf; Tf, transferrin; Tf-R, Tf receptor; Tx, Texas-red; Tx-Tf, Texas-red-labeled Tf.

Please address all correspondence to Dr. F.R. Maxfield, Department of Pathology, Rm 15-420, College of Physicians and Surgeons, Columbia University, 630 West 168th Street, New York, NY 10032.

somally directed molecules are retained; or (2) by a default process in which membrane receptors are recycled along with most of the membrane components while acid-released ligands are lysosomally directed along with the luminal content of the sorting endosome. The two possibilities are not mutually exclusive. However, singly, they lead to very different testable predictions.

In the first case, it has been proposed that recycling receptors are specifically concentrated in tubular extensions of the sorting endosome (or the compartment for the uncoupling of ligand and receptor, [CURL]; Geuze et al., 1983) and that the targeting of these structures towards the recycling pathway results in sorting. This could be achieved by molecular recognition signals such as peptide sequences involved in the retrieval of recycling components. No recognition signals for recycling have been identified, but some evidence in support of specific retrieval of membrane receptors has been obtained in rat liver cells, where recycling asialoglycoprotein receptors appear to be at higher concentrations in the tubular extensions of the sorting endosome (or CURL; Geuze et al., 1987).

In the second case, the geometry of the tubular-vesicular sorting endosome has been considered as a possible mechanism for such a 'default' sorting process (Dunn et al., 1989; Linderman and Lauffenburger, 1988; Rome, 1985). A prediction of the geometric (default) basis for sorting is that bulk membrane, carrying no specific signals other than membrane association, would be efficiently recycled along with membrane-associated receptors, while bulk volume content consisting of the acid-released ligands would be lysosomally destined. On the other hand, if specific signals are required for recycling of receptors, bulk membrane would not traverse the recycling pathway with similar rates and efficiency as receptors. Comparison of the endocytic route and the kinetics of trafficking of bulk membrane with a recycling receptor in morphological and kinetic analyses performed in the same cell would directly address this issue.

Koval and Pagano have studied the endocytic trafficking and metabolism of a membrane-lipid analog, *N*-[*N*-(7-nitro-2,1,3-benzoxadiazol-4-yl)-ε-aminohexanoyl]-sphingosylphosphorylcholine (C_6-NBD-SM) (for review see Koval and Pagano, 1991). They found that C_6-NBD-SM was endocytosed in compartments that contain fluorescently labeled Tf. Using whole-cell kinetic measurements they showed that a majority (>95%) of the internalized lipid is efficiently recycled (Koval and Pagano, 1989) while only a small fraction of the endocytosed lipid is delivered to lysosomes (Koval and Pagano, 1990). However, it is not known whether C_6-NBD-SM and recycling receptors follow the same endocytic route with similar kinetics.

In this report we show that C_6-NBD-SM enters the endocytic system as a bulk membrane marker, and its endocytic route is kinetically and morphologically identical to fluorescently labeled Tf. The lipid analog rapidly sorts from lysosomally directed molecules in the sorting endosome and accumulates in the recycling compartment before recycling back to the cell surface.

Materials and Methods

Cell Cultures

All experiments were carried out using TRVb-1 cells, a line of CHO cells lacking hamster Tf-R and transfected with a human Tf-R, or another CHO cell line (WTB111 cells; Robbins et al., 1984) containing the hamster receptor, and cultured as described previously (McGraw et al., 1987). 3 days before each experiment, cells were plated on 35-mm diameter coverslip bottom dishes (Salzman and Maxfield, 1989) and used at 50–80% confluency for microscope experiments and 80–90% confluency for biochemical experiments.

Fluorescent Labels

Human transferrin (Sigma Chem. Co., St. Louis, MO) was iron-loaded and purified by Sephacryl S-300 (Pharmacia LKB, Uppsala, Sweden) gel-filtration chromatography and conjugated to rhodamine isothiocyanate or FITC as previously described (Yamashiro et al., 1984). Cy3™ (Biological Detection Systems, Pittsburgh, PA) or Texas-red™ (Molecular Probes Inc., Eugene, OR) conjugated proteins were made according to the manufacturers' instructions. The conjugation was carried out at 3 mg/ml protein concentration and at 0.5 mg/ml dye concentration. The final dye to protein ratio was routinely determined to be between 1.0 and 1.3. 3,3'-dioctadecyloxacarbocyanine- and 3,3'-dioctadecylindocarbocyanine-labeled LDL (DiO-LDL and DiI-LDL, respectively) were prepared according to (Pitas et al., 1981) and provided by Drs. J. N. Myers and I. Tabas (Columbia University, NY). C_6-NBD-SM and C_6-NBD-PC were obtained from Molecular probes and purified by thin layer chromatography before use. C_6-NBD-galactosylceramide was prepared according to published procedures (Kishimoto, 1975) from C_6-NBD-fatty acid (Molecular Probes) and psychosine (Sigma Chem. Co.) and purified by thin layer chromatography as described previously (van Meer et al., 1987).

C_6-NBD-lipid vesicles (100 μM total lipid) were prepared according to Kremer et al. (1977) by injecting an ethanolic solution (2.5 mM total lipid concentration) consisting of a mixture (1:1 or 2:3) of C_6-NBD-lipid and dioleylphosphatidylcholine (Avanti Polar Lipids Inc., Albaster, AL), into 150 mM NaCl, 20 mM Hepes, pH 7.4. Ethanol (<8%) was removed by dialysis into 150 mM NaCl, 20 mM Hepes, pH 7.4, 5 mM KCl and the resulting vesicle solution was stored in the dark, under argon at 4°C.

Fluorescent Labeling of Cells

TRVb-1 cells were incubated for 30 min at 0°C with the fluorescently labeled protein, in Hepes-buffered (20 mM, pH 7.3) Hams F-12 media including 10 mM $NaHCO_3$ (HF-12) in the presence of 2 mg/ml ovalbumin (HF-12-Ova) or without ovalbumin as indicated. The cells were warmed to 37°C for the indicated periods. At the end of the incubation period the cells were rinsed (5 × 2 ml) with ice cold Med 1 (150 mM NaCl, 20 mM Hepes, pH 7.4, 5 mM KCl, 1 mM $CaCl_2$, 1 mM $MgCl_2$) containing >1 mg/ml of excess unlabeled ligands, fixed in 2% paraformaldehyde in Med 1 at 0°C for 10 min, and taken for fluorescence microscopy. In some cases the cells were fixed at room temperature in 2% paraformaldehyde in PBS for 30 min. In pulse-chase experiments the cells were chased in Med 1 containing 5 g/l glucose, 1× MEM amino acids (GIBCO BRL, Gaithersburg, MD), 1% BSA and 10 μM deferoxamine mesylate (Sigma Chem. Co.), and 1 mg/ml unlabeled protein ligand, before fixation as above.

Lipid labeling of TRVb-1 cells was accomplished by incubating the cells at 0°C with C_6-NBD-lipid vesicles at the indicated concentrations for 30 min in HF-12. After labeling, the cells were washed extensively in ice cold HF-12 (5 × 2 ml). The cells were then warmed up to 37°C for the indicated periods, back-exchanged in 5% BSA in Med 1 (6 × 5 min changes) to remove surface C_6-NBD-lipid, and fixed as described above. The back-exchange procedure removed at least 98% of cell surface–associated lipid. To rule out that quantitative fluorescence microscopic analyses of intracellular labeling of organelles may be complicated by hydrolysis of C_6-NBD-SM (Koval and Pagano, 1989), biochemical analyses of C_6-NBD-SM metabolism were carried out (see below). Under the conditions of the pulse and chase conditions used in the experiments described in this report, <5% of the total cell-associated C_6-NBD-SM was converted to C_6-NBD-ceramide, and no C_6-NBD-glucosylceramide was detected even at the longest chase times.

Quantitative Fluorescence Microscopy

Images of fluorescently labeled cells were obtained by two independent means, video recording of an intensified signal collected via a video camera, described in Maxfield and Dunn (1990) or via a charged-coupled device (CCD) equipped camera.

DiO-LDL and Rh-Tf fluorescence images were recorded from the same field using different filter sets. Rhodamine-labeled Tf (Rh-Tf) fluorescence was visualized using a Leitz fluorescence microscope equipped with a 63×,

NA 1.4 objective or 40×, NA 1.3 objective (Leitz Wetzlar, Germany) and a 530–560-nm band pass excitation filter, a 580-nm dichroic mirror, and a 580-nm long pass emission filter. FITC-T_f and DiO-LDL were visualized with the same equipment but a 450–490-nm band pass excitation filter, a 510-nm dichroic mirror, and a 515–545-nm band pass emission filter were used. NBD-fluorescence images were obtained using the same optics described for DiO-LDL. DiI or Cy3 fluorescence images were recorded using the Rhodamine filter set. Texas red-fluorescence images were recorded using the same equipment but a Texas red filter set (540–580 nm band pass excitation filter, a 595-nm dichroic mirror, and a 600-nm long pass emission filter) was used to visualize the fluorescence. In some cases NBD and Texas red–labeled samples were imaged using a FITC/Texas red dual dichroic filter set while NBD and DiI, or Cy3-labeled samples were imaged using a FITC/TRITC dual dichroic filter set. All optical filters were image quality and purchased from Omega Optical (Brattleboro, VT).

Video images were recorded on a JVC CR6650U video cassette recorder with a Videoscope KS1380 image intensifier coupled to a VS2000N video camera. Neutral density filters (5, 13, 33% transmission) were used to keep the fluorescence intensities from exceeding the camera's linear range.

A cooled CCD camera (Photometrics, Inc., Tuscon, AZ), equipped with a KAF 1400 mega-pixel Kodak chip was used to record time-integrated images of NBD-fluorescence (Hirschfeld, 1976; Jovin and Arndt-Jovin, 1989). In this method, all the NBD-fluorescence was collected until the sample was completely photobleached. Texas red images from the same field were collected over a shorter length of time of obtain adequate Texas-red fluorescence images, after refocusing in phase-contrast optics to the same focal plane from which the NBD-image was obtained. The expanded dynamic range of the CCD camera (~12 bits) compared to the intensified video camera (~8 bits) allowed the visualization of time-integrated fluorescence NBD-images; neutral density filters (10, 25, or 50%) were used in the emission light path to compensate for different labeling conditions. Crossover of Texas-red fluorescence into the NBD-channel was found to be undetectable. NBD-fluorescence crossover into the Texas-red channel was not observed because the time-integrated fluorescence emission method completely photobleaches the NBD-fluorophore.

Image Processing

Video images were processed as described previously (Dunn et al., 1989; Maxfield and Dunn, 1990; Mayor and Maxfield, 1993). In a preliminary report (Mayor and Maxfield, 1993), we have used video camera fluorescence microscopy to measure the accumulation kinetics of C_6-NBD-SM and Texas-red–labeled Tf (Tx-Tf) in sorting endosomes. Although similar results as described in Fig. 5 were obtained, instantaneous fluorescence measurements (video camera images) of the NBD-fluorophore may lead to erroneous estimates of total fluorescence due to the rapid photobleaching and/or concentration-dependent self-quenching properties of C_6-NBD-SM inserted in lipid-bilayers (Nichols and Pagano, 1981; and unpublished observations). Time-integrated fluorescence is independent of the quantum efficiency of the fluorophore (Hirschfeld, 1976) thus, the time-integrated fluorescence photobleaching method overcomes these technical pitfalls and allows accurate and sensitive quantitation of total fluorescence (Jovin and Arndt-Jovin, 1989). In the experiments described in this report, time-integrated emission of NBD-fluorescence was used to make quantitative measurements of NBD-fluorescence using a CCD camera.

CCD images were processed using a SPARC station 4/330 computer system (Sun Microsystems Inc., Mountainview, CA) and image processing software provided by Inovision Corp. (Durham, NC). Image processing routines, outlined in Dunn et al. (1989) and Maxfield and Dunn (1990), were adapted for use on the SPARC workstation. Briefly, the digitized images were background corrected (Maxfield and Dunn, 1990) and sorting endosomes were defined by size (4–40 pixels in area; 1 pixel = 0.14 μm, at 63× magnification) and shape of intensity profile (Dunn et al., 1989).

In some experiments (see Fig. 7), the recycling compartments in each image (obtained at 63×, NA 1.4) were defined by obtaining a mask image from the corresponding median-filtered Tx-Tf images, consisting of large fluorescent spots (>125 pixels in area), with brightness greater than one half the brightest value in each spot of contiguous pixels. By visual inspection this procedure was found to be satisfactory because it identified all (>90%) the recycling compartments and did not include any sorting endosomes. A constant cellular background was subtracted from the raw images, and the recycling compartments in each field were selected using the corresponding Tx-Tf mask image. The ratios of NBD to Texas-red fluorescence were then determined independently for each recycling compartment. In other experiments (see Fig. 8), the images were obtained using a 40×, NA 1.3, objective lens, and processed using a modified procedure. The images were initially background subtracted (median-filtered background images were obtained using a neighborhood size of 128 pixels) and all contiguous pixels, with intensity greater than one third the brightest value in each spot, were retained. The recycling compartments in each field were directly defined by selecting an appropriate minimum pixel-size (100 pixels in area; 1 pixel = 0.205 μm, at 40× magnification) as a cut-off. In all cases the recycling compartment colocalized for each of the two labels, and did not contain sorting endosomes.

Biochemical Procedures for NBD-Lipid Quantitation

Total amount of C_6-NBD-SM transferred to cells during the 30 min surface-labeling procedure was quantified as described previously (Koval and Pagano, 1989). Briefly, cells were labeled at 0°C with different concentrations of C_6-NBD-SM-labeled vesicles and rinsed five times with ice cold Med 1. The cells were then incubated in 2.5 mM EDTA in PBS for an additional 15 min at 0°C and scraped into Eppendorf tubes in a final volume of 0.8 ml. An aliquot (80 μl) was taken for DNA analysis (Labarca and Paigen, 1980) and the remaining sample extracted twice with an equal volume of butanol. The butanol extracts were subjected to fluorimetric analysis for the presence of NBD fluorescence (λ_{ex} = 470 nm; λ_{em} = 520–540 nm) using a fluorimeter (SLM 8000, SLM Instruments, Inc., Urbana, IL).

Assessment of cellular metabolism of C_6-NBD-SM was carried out by thin layer chromatographic analyses of NBD-lipids present in the cell and/or medium during the pulse and chase conditions used in the experiments described above. These methods are described in detail elsewhere (Presley, J. F., S. Mayor, K. W. Dunn, L. S. Johnson, T. E. McGraw, and F. R. Maxfield, manuscript submitted for publication), and are based on methods described earlier (Koval and Pagano, 1989).

Results

Morphological Analyses of Intracellular Trafficking of Fluorescently Labeled Tf, LDL, and Lipid in CHO Cells

When FITC-T_f and DiI-LDL are endocytosed via receptor mediated endocytosis in CHO cells that express a transfected human Tf-R TRVb-1 cells, they are initially colocalized in peripherally located organelles, the sorting endosomes (punctate structures in Fig. 2, *A* and *C*; Dunn et al., 1989). We have frequently observed that in some cases the centers of Tf fluorescence do not exactly coincide with the corresponding LDL fluorescence in the same structure, even at these early times. FITC-T_f and DiI-LDL then rapidly sort from each other (Fig. 2, *B* and *D*). FITC-T_f exits the peripherally located punctate endosomes and accumulates in the peri-centriolar region of the cell in the recycling endosomal compartment (Fig. 2, *B* and *D*) while DiI-LDL remains in punctate endosomes. Similar results have been previously obtained with Tf and α_2M: Tf rapidly sorts from α_2M and accumulates in the recycling compartment while α_2M is delivered to late endosomes (Salzman and Maxfield, 1989; Yamashiro et al., 1984).

As shown in Fig. 3, when Tx-Tf and C_6-NBD-SM are cointernalized they showed a complete colocalization of fluorescence patterns during the entire period of accumulation and chase; appearing first in peripheral (punctate) sorting endosomes (Fig. 3, *A* and *C*) and rapidly exiting these organelles to accumulate in the recycling compartment (Fig. 3, *B* and *D*). To observe sorting of labeled lipid from a probe that accumulates in sorting endosomes, we carried out pulse-chase studies with C_6-NBD-SM and Cy3-labeled α_2M (Cy3-α_2M) as described in Fig. 2 for Tf and LDL. C_6-NBD-SM was observed to leave the sorting endosomes containing Cy3-α_2M in a process indistinguishable from the sorting of Tf from LDL (data not shown). Similar to the results ob-

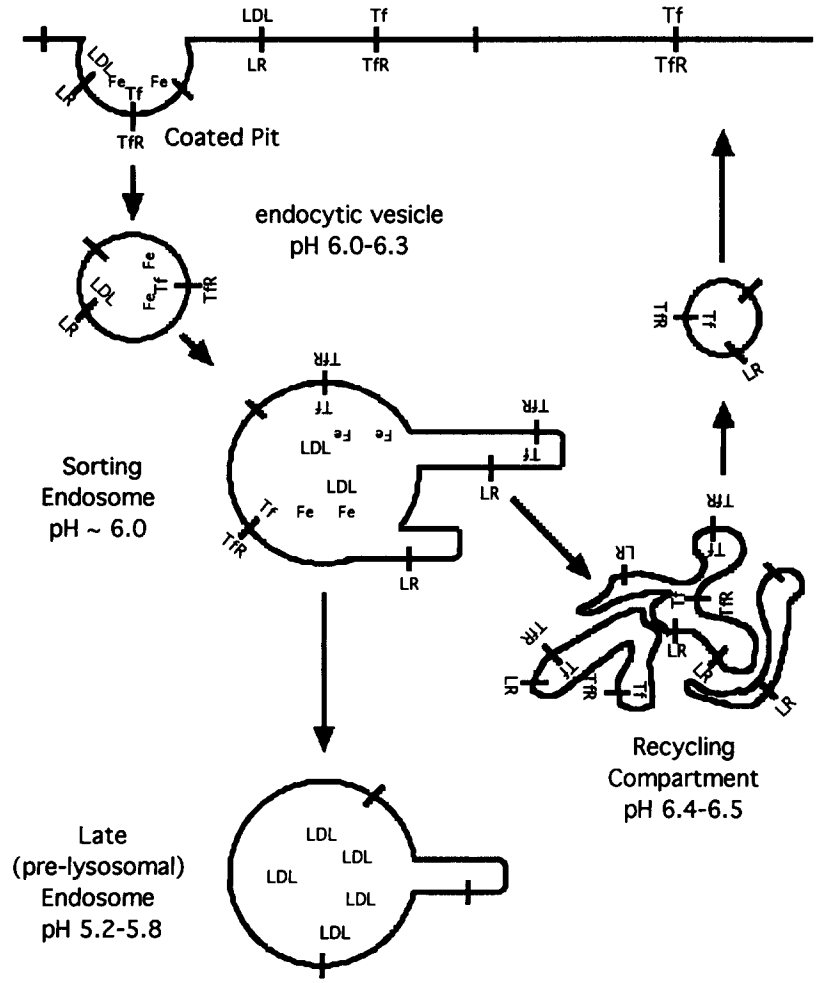

Figure 1. Schematic of endocytic process. This schematic illustrates various fates of internalized molecules, diferric transferrin ($^{Fe}Tf^{Fe}$) and *LDL* and their receptors, *TfR* and *LR*, respectively. *LDL* is released from *LR* in the acidic milieu of endosomes. *LR* is then recycled back to the surface. Internalized *LDL* is eventually delivered to lysosomes. $^{Fe}Tf^{Fe}$ also releases its bound iron in an early endosomal compartment. Apo-transferrin (*Tf*), at the acidic pH of endosomes, remains associated with *TfR* and is recycled back to the plasma membrane via a peri-centriolar recycling compartment. This sorting of recycled molecules from lysosomally destined molecules takes place in tubulo-vesicular endosomes, referred to as sorting endosomes. Recycling molecules then accumulate in the recycling compartment en route to the cell surface. The late endosome represents a compartment that contains endocytosed molecules destined for the lysosome but not recycling receptors, *LRs*, or *TfRs*.

tained by Koval and Pagano (1989), we have been unable to detect delivery of C_6-NBD-SM to late endosomes or lysosomes.

To make sure that this sorting was not specific for sphingomyelin, we carried out studies with a fluorescent phosphatidylcholine analog, C_6-NBD-phosphatidylcholine (C_6-NBD-PC) and a neutral sphingolipid analog, C_6-NBD-galactosylceramide. When Tx-Tf and either one of the C_6-NBD-lipids were internalized in TRVb-1 cells, the labeled markers were initially in colocalized, peripherally located sorting endosomes, and then appeared to accumulate with similar kinetics in the recycling compartment (data not shown). Qualitative inspection of several fields strongly suggests that Tx-Tf, C_6-NBD-PC, and C_6-NBD-galactosylceramide also traverse morphologically and kinetically identical pathways in these cells. However, the rapid rate of hydrolysis of C_6-NBD-PC under the incubation conditions used in these experiments and during microscopic imaging (data not shown) prevented quantitative analyses of C_6-NBD-PC trafficking. In pulse chase studies similar to those shown in Fig. 3, when Tx-Tf and C_6-NBD-galactosylceramide (which was stable under the experimental conditions used) were internalized they showed a complete colocalization of fluorescence patterns during the entire period of accumulation and chase (data not shown). With similar kinetics, the two labeled markers appeared first in sorting endosomes and rapidly exited these organelles to accumulate in the recycling compartment, and finally exited the cell. This confirmed that this sorting towards the recycling pathway was not specific to C_6-NBD-SM. Further detailed quantitative analyses presented in this report were performed only with C_6-NBD-SM.

In the following sections we have used quantitative fluorescence microscopy to compare kinetics of Tx-Tf and C_6-NBD-SM trafficking during endocytosis.

Concentration Dependence of C_6-NBD-SM–labeled Endosome Fluorescence

To confirm that C_6-NBD-SM is internalized as a bulk membrane marker, we measured the increase in sorting endosome fluorescence with increasing C_6-NBD-SM incorporated in the plasma membrane. As described in Materials and Methods, sorting endosomes were identified as punctate spots consisting of 4–40 pixels (mean area was typically 8–10 pixels) that were peripherally located and did not overlap with the large peri-centriolar fluorescent area. Fig. 4 shows that sorting endosome fluorescence increased proportional to C_6-NBD-SM vesicle concentration in the labeling medium, identical to the linear increase in plasma-membrane lipid concentration observed over a similar range of

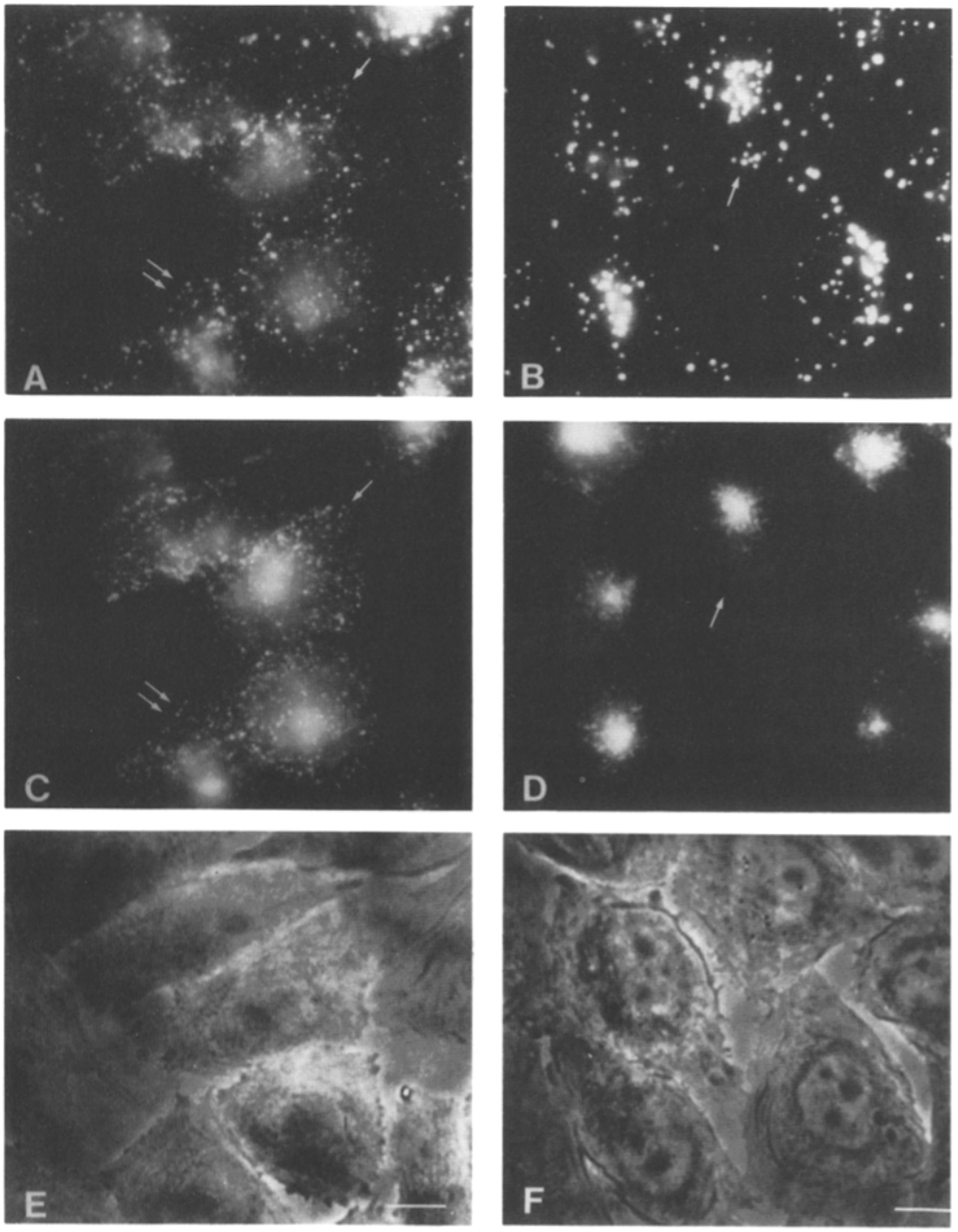

Figure 2. Sorting of LDL and Tf in CHO cells. TRVb-1 cells were labeled at 4°C for 20 min with DiI-LDL (2 μg/ml) and 25 μg/ml FITC-T_f in HF-12 containing 1 mg/ml ovalbumin, pulsed for 2 min at 37°C, and cooled to 4°C with ice-cold Med 1 and the surface-fluorescence removed as described in Materials and Methods. The pulsed cells were chased for 0 min (*A* and *C*) or 5 min (*B* and *D*) at 37°C in Med 1 containing 1 mg/ml ovalbumin, 1 mg/ml unlabeled Tf, and 10 μM deferoxamine and fixed in 2% paraformaldehyde at room temperature for 30 min. DiI-LDL fluorescence images (*A* and *B*) and FITC-T_f fluorescence images (*C* and *D*) were recorded from the same field of cells using a 63×, NA 1.4, objective, appropriate filters including a dual-dichroic, a CCD camera, and photographed off the video monitor. Arrows are intended as landmarks to guide the reader. Phase-contrast images are shown in *E* and *F*.

C_6-NBD-SM vesicle concentration. This linear increase in sorting endosomal fluorescence is consistent with C_6-NBD-SM being internalized via a bulk process wherein the amount of internalized lipid is directly proportional to the concentration of the lipid introduced into the plasma membrane. These data also show that the time-integrated fluorescence method used in these analyses is capable of accurately quantifying an increase in endosome fluorescence due to increased C_6-NBD-SM being delivered to the sorting endosome.

Intracellular Accumulation of Fluorescently Labeled Tf, DiI-LDL, and C_6-NBD-SM in Sorting Endosomes

To determine the kinetics of accumulation of Tf and LDL in sorting endosomes, TRVb-1 cells were incubated for different lengths of time in the continuous presence of DiO-LDL and Rh-Tf, and the geometric mean of endosome brightness was determined for DiO-LDL–labeled and Rh-Tf–labeled sorting endosomes in the same cells. The mean endosome brightness of DiO-LDL–containing endosomes continued to increase for the duration of the pulse. However, in the corresponding Rh-Tf–labeled endosomes mean endosome brightness came to a steady state rapidly, within 2–3 min (Fig. 5 *A*). Similar results were reported by Dunn et al. (1989). When Tx-Tf and C_6-NBD-SM were pulsed into the cell for the indicated periods and the mean endosome brightness was measured at different times during the pulse, the two fluorescently labeled molecules rapidly and simultaneously came to steady state in sorting endosomes (Fig. 5 *B*). A separate analysis of the data showed that the total Tx-Tf or C_6-NBD-SM fluorescence in sorting endosomes per cell also came to a steady state with identical kinetics (data not shown).

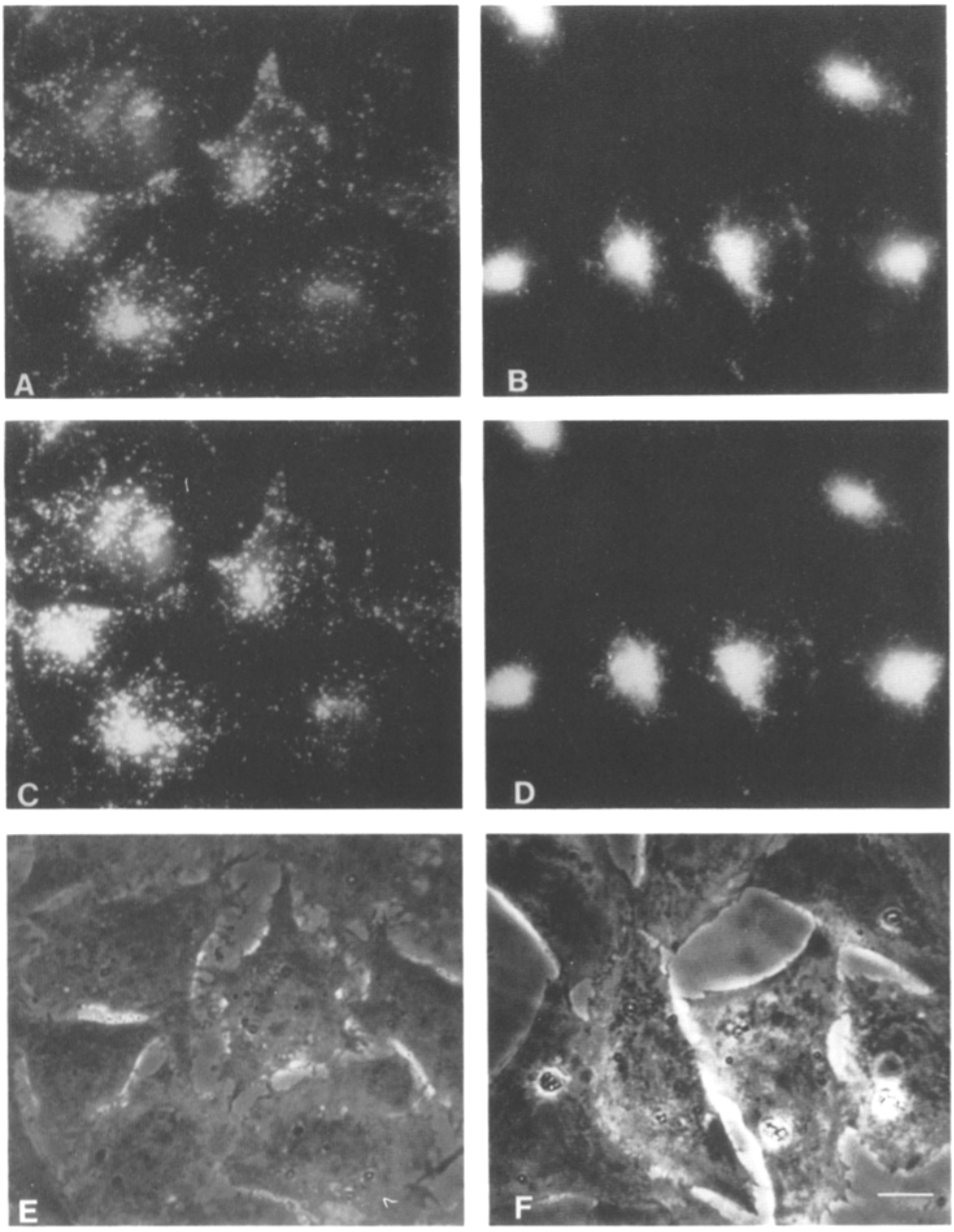

Figure 3. Exit of C_6-NBD-SM and Tx-Tf from sorting endosomes and accumulation of the two molecules in the recycling compartment. TRVb-1 cells were labeled at 4°C with C_6-NBD-SM vesicles (3 μM total lipid) and 25 μg/ml Tx-Tf, incubated for 2.5 min at 37°C, back exchanged and chased for 0 min (*A* and *C*) or 6 min (*B* and *D*) at 37°C in HF-12 containing 1% BSA, 10 μM deferoxamine, and 1 mg/ml unlabeled Tf. Time-integrated NBD-fluorescence images (*A* and *B*) and Tx-Tf fluorescence images (*C* and *D*) were recorded using a 63× objective and a CCD camera, and photographed off the video monitor at similar gray-scale levels for *A* and *B*, and *C* and *D*. Phase-contrast images are shown in *E* and *F*.

During a continuous pulse experiment, in the presence of saturating amounts of fluorescent-Tf in the labeling medium and a large pool of cell-surface incorporated C_6-NBD-SM, kinetic modeling of accumulation kinetics show that the rate of approach to steady state in the sorting endosomes will be governed mainly by the rate of exit from the sorting endosome. Thus, the data suggest that Tf and C_6-NBD-SM are rapidly and simultaneously removed from sorting endosomes while LDL continues to accumulate in these endosomes.

Exit of C_6-NBD-SM and Tx-Tf from Sorting Endosomes and Arrival in the Recycling Compartment

When C_6-NBD-SM and Tx-Tf were pulsed into cells for a short period (2 min) and chased for different lengths of time in the absence of labeled molecules in the chase medium or plasma membrane, the two molecules were first detected in peripherally located sorting endosomes, and then in the recycling compartment located in the peri-centriolar region of the cell (see Fig. 3). Quantitative analysis of the rate of exit of C_6-NBD-SM and Tx-Tf from the sorting endosomes is shown in Fig. 6. The two molecules leave these endosomes with identical rates ($t_{1/2}$ ~2.5 min). During the entire time course of the pulse and chase period there was extensive colocalization of the two fluorescent patterns; >80% of the total fluorescence in sorting endosomes in each image colocalized with the other fluorescent probe.

Using the same double-labeled cells, a more sensitive assay of any difference in kinetics was obtained by determining

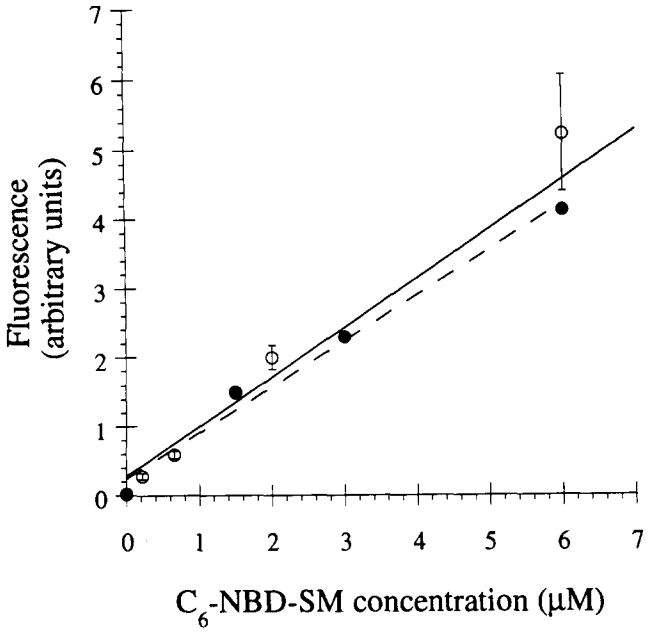

Figure 4. Concentration dependence of endosome fluorescence. TRVb-1 cells were surface labeled as described in Fig. 3 at the indicated concentrations of C_6-NBD-SM vesicles and the total amount of lipid transferred to the cells (*open circles*) was determined spectrophotometrically and normalized to the DNA content as described in Materials and Methods. The data shown are the average values (±SD) obtained from three separate 6-cm dishes. Plasma membrane-associated C_6-NBD-lipid increased directly proportional to the increase in concentration of C_6-NBD-SM vesicles in the labeling medium, similar to results described by Koval and Pagano (1989). Independently labeled cells in coverslip dishes were pulsed for 3 min after labeling with C_6-NBD-SM vesicles at the indicated concentrations, back-exchanged, and analyzed by quantitative fluorescence microscopy as described in Materials and Methods. Total endosome fluorescence (*closed circles*) was determined as the sum of fluorescence in punctuate endosomes (structures between 4 and 40 pixels) and normalized to the number of nuclei in each field. Fluorescence at each concentration (determined either spectrophotometrically or by quantitative fluorescence microscopy) was normalized to the value obtained at the lowest concentration of lipid used in each case.

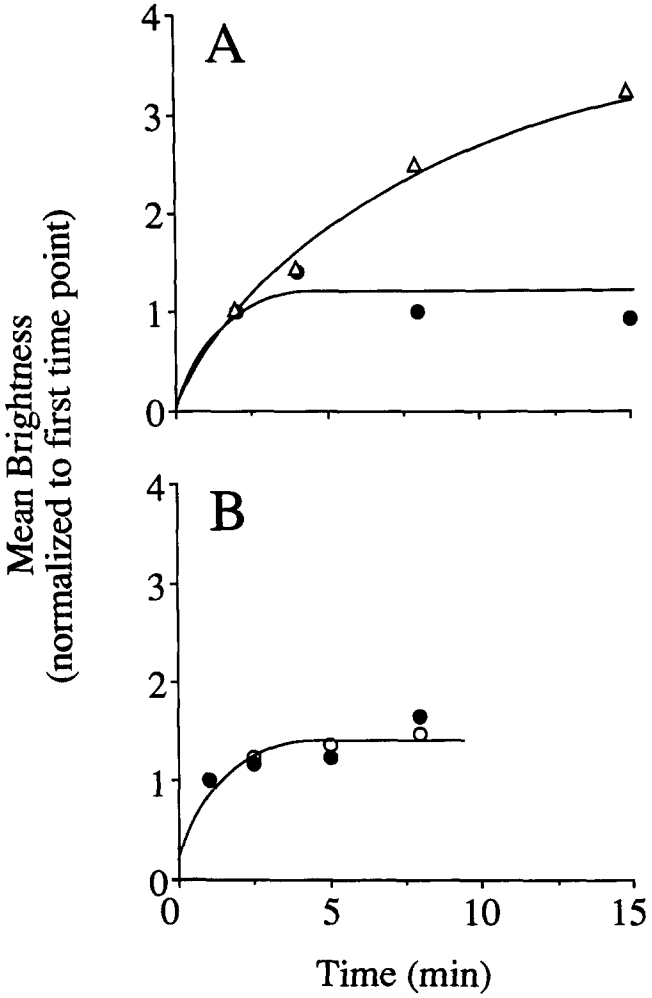

Figure 5. Time course of accumulation of DiO-LDL, C_6-NBD-SM, and fluorescent-Tf in sorting endosomes. Mean brightness of endosomes labeled with DiO-LDL and Rh-Tf (*A*), or Tx-Tf and C_6-NBD-SM (*B*) at the indicated times were measured during a continuous pulse of label. In *A*, Rh-Tf (*filled circles*) and DiO-LDL (*open triangles*) images were recorded using a video-camera. In *B*, C_6-NBD-SM (*open circles*) and Tx-Tf (*filled circles*) images were obtained using a CCD camera, and mean endosome brightness was determined as described in Materials and Methods. The data show that DiO-LDL continues to accumulate in sorting endosomes while both C_6-NBD-SM and fluorescent-Tf rapidly (within 2–3 min) reach a steady state level of mean endosome brightness in the same organelles. The data points shown are the geometric mean of measured endosome brightness of 8–12 fields of 3–8 cells each, corresponding to 2,000–5,000 endosomes/data set. The mean values were normalized to the first time point in each case (2-min endosomes, *A*; 1-min endosomes, *B*). Standard errors from the mean are in each case smaller than the size of the symbol.

the ratio of C_6-NBD-SM-fluorescence to Tx-Tf in sorting endosomes at different times during the chase period (Fig. 7). The ratio of total C_6-NBD-SM to total Tx-Tf fluorescence in sorting endosomes remained constant over the entire chase period confirming that the two probes leave the collection of sorting endosomes with identical kinetics. The distribution of ratios of C_6-NBD-SM and Tx-Tf fluorescence in individual sorting endosomes also remained constant during the entire chase period (data not shown), suggesting that the lipid and protein markers exited individual sorting endosomes at similar rates.

We then measured the ratio of C_6-NBD-SM to Tx-Tf fluorescence in the pericentriolar recycling compartment in the cells analyzed above and found that this ratio was also constant during this chase period (Fig. 7). Since the pulse and chase conditions used here are relatively short compared to the rate of exit of C_6-NBD-SM and Tx-Tf from the recycling compartment (see below), the constancy of the ratios in the recycling compartment shows that C_6-NBD-SM and Tx-Tf accumulate in the recycling compartment with identical kinetics.

The ratio of C_6-NBD-SM to Tx-Tf fluorescence in the recycling compartment was found to be equal to that in the sorting endosomes at each time point. The equivalence of the fluorescence ratios in the sorting endosomes and the recycling compartment in three separate experiments is shown in

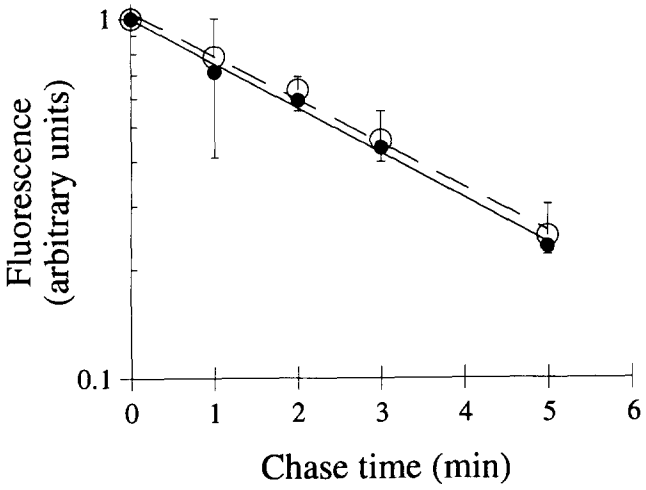

Figure 6. Kinetics of exit of C_6-NBD-SM and Tx-Tf from sorting endosomes. TRVb-1 cells were labeled at 4°C with C_6-NBD-SM (3 μM total lipid) and Tx-Tf (25 μg/ml), incubated for 2.5 min at 37°C, back exchanged, and incubated for an additional 2 min at 37°C in HF-12 to internalize any remaining cell-surface lipid and transferrin. The cells were then chased for the indicated lengths of time, fixed, and fluorescence images (5–6 fields; 3–10 cells/field) were recorded as described in Fig. 3. Total fluorescence in C_6-NBD-SM (*open circles*) and Tx-Tf (*closed circles*) sorting endosomes (containing both labels) at each chase point was determined as described in Materials and Methods, and normalized to the number of nuclei at each time point. The data presented are an average of two separate experiments. The data were fitted to single exponentials, $y = 1.00e^{(-0.29x)}$ ($R = 0.99$) for C_6-NBD-SM, and $y = 1.04e^{(-0.28x)}$ ($R = 0.99$) for Tx-Tf, to determine the rate of exit of the two molecules from sorting endosomes. These rates correspond to $t_{1/2}$ s of 2.45 min and 2.47 min for C_6-NBD-SM and Tx-Tf, respectively.

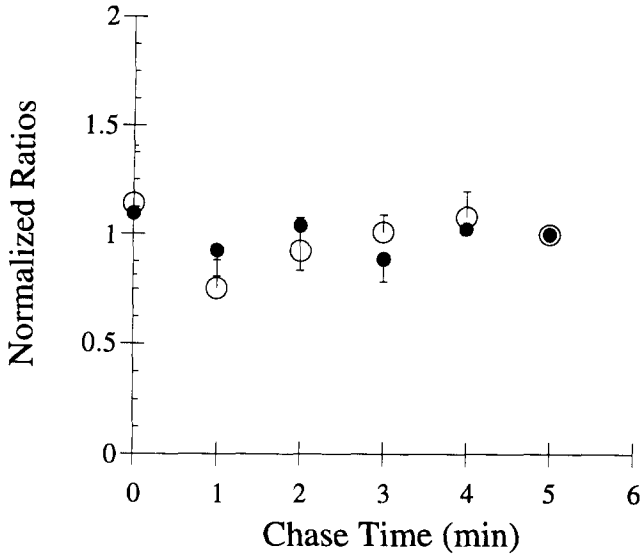

Figure 7. Ratio of C_6-NBD-SM and Tx-Tf fluorescence in the various compartments of TRVb-1 cells. Double-labeled cells as described in Fig. 6 were analyzed for the ratios of C_6-NBD-SM and Tx-Tf fluorescence in sorting endosomes (*filled circles*) and recycling compartment (*open circles*) as described in Table I. The ratios in the sorting endosomes at the indicated chase times were determined by dividing the total sorting endosome fluorescence for each label. The corresponding ratios in the recycling compartment are the geometric means of the ratios in individual recycling compartments. Each data point shown above is the average (±SD) of normalized ratios from three separate experiments. The ratios at each time point in a single experiment were normalized to the ratio at the end of the chase ($t = 5$ min). The average ratios in each experiment are shown in Table I.

Table I. Fig. 7 and Table I demonstrate that the average ratios determined from many fields at each chase time for C_6-NBD-SM and Tx-Tf fluorescence in sorting endosomes and the recycling compartment are constant and equal to each other. To make sure that even at the single cell level, C_6-NBD-SM and Tx-Tf fluorescence ratios in the two endosomal compartments were similar to each other, we examined the ratios of C_6-NBD-SM to Tx-Tf fluorescence in sorting endosomes and recycling compartment in the same cell. We found that total C_6-NBD-SM to Tx-Tf fluorescence ratios in sorting endosomes and the recycling compartment were within 10–15% of each other for all cells examined at all chase times (5–8 cells were examined per time point).

These analyses show that C_6-NBD-SM and Tx-Tf not only leave the sorting endosomes and accumulate in the recycling compartment with identical kinetics but also arrive in the same proportion to each other in the recycling compartment.

Table I. Average Ratios of C_6-NBD-SM to Tx-Tf Fluorescence*

Expt No.	Sorting endosomes‡	Recycling compartment§
1	0.77 ± 0.12	0.86 ± 0.188
2	0.56 ± 0.049	0.55 ± 0.089
3	0.60 ± 0.083	0.63 ± 0.083

* The average ratios (±SD) for each experiment were obtained from the fluorescence ratios determined at chase times shown in Fig. 7.

‡ Ratios of C_6-NBD-SM to Tx-Tf fluorescence in sorting endosomes were obtained by determining the total fluorescence of each label in the sorting endosomes at the indicated chase times.

§ Recycling compartment ratios were obtained from the same fields as described above, as the mean of fluorescence ratios in individual recycling compartments at each chase time. Individual recycling compartment ratios were obtained by dividing the total fluorescence in a mask area encompassing a region within the peri-centriolar recycling compartment, of equal size for the C_6-NBD-SM and Tx-Tf–labeled compartments, as described in Materials and Methods.

Exit of C_6-NBD-SM and Tx-Tf from the Recycling Compartment

To make comparative measurements of the exit of C_6-NBD-SM and Tx-Tf from the recycling compartment, the two markers were pulsed into TRVb-1 cells for 10 min and chased as described in Materials and Methods. Total fluorescence in the recycling compartment at each chase point was determined, and the data were fitted to single exponentials as shown in Fig. 8 *A*. The rates of exit of C_6-NBD-SM and Tx-Tf from this compartment were found to be within experimental error, with $t_{1/2}$s of ~9.5 min and ~8.5 min, respectively. The mean ratios of C_6-NBD-SM and Tx-Tf fluorescence in individual recycling compartments were determined at each time point and found to be constant throughout the chase period (Fig. 8 *B*).

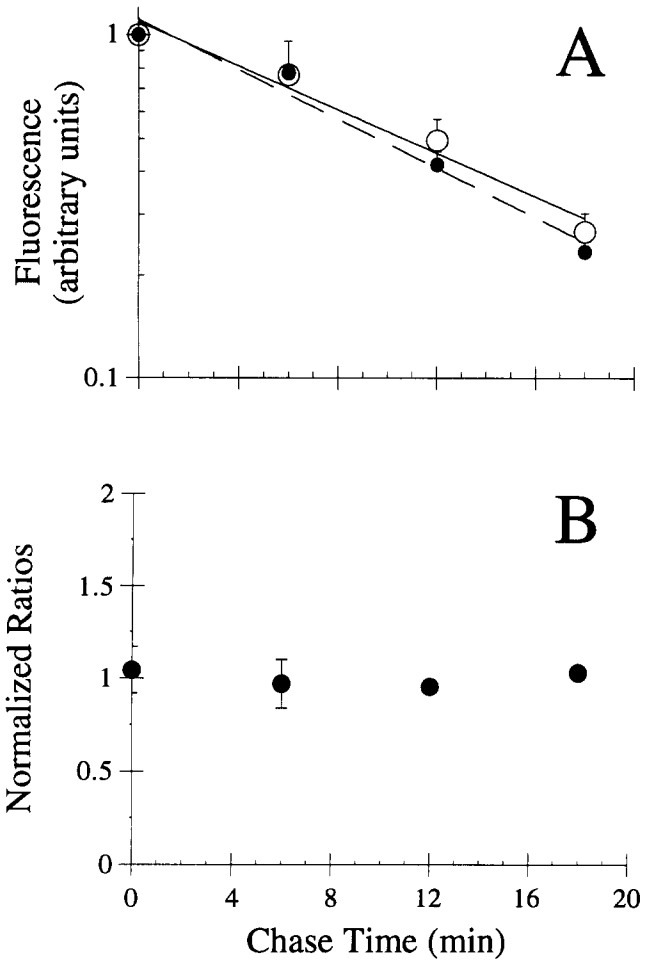

Figure 8. Kinetics of exit of C_6-NBD-SM and Tx-Tf from the recycling compartment. (*A*) TRVb-1 cells were labeled at 4°C with C_6-NBD-SM (3 μM total lipid conc.) and Tx-Tf (25 μg/ml), incubated for 10 min at 37°C, back exchanged, and incubated for an additional 6 min at 37°C in HF-12 to chase any remaining lipid and transferrin into the recycling compartment. The cells were then chased as described in Fig. 6 for the indicated times. The fluorescence images (5–6 fields; 5–15 cells/field) were recorded as described in Fig. 6 except that a 40×, NA 1.3 objective was used to collect the images. The images were processed as described in Materials and Methods. Total fluorescence in the recycling compartment for each time point was determined after eliminating the small punctate spots (< 100 pixels) from each field. The data was normalized to the number of nuclei at each time point and to the 0-min chase point value, and presented as an average of two separate experiments. The data were fitted to single exponentials $y = 1.09e^{(-0.073x)}$ ($R = 0.98$) for C_6-NBD-SM (*open circles*), and $y = 1.11e^{(-0.083x)}$ ($R = 0.97$) for Tx-Tf (*closed circles*) for the rate of exit of the two molecules from the recycling compartment. These rates correspond to $t_{1/2}$ s of 9.5 min and 8.3 min for C_6-NBD-SM and Tx-Tf, respectively. (*B*) The fluorescence ratios in the recycling compartment at the indicated chase times were determined by obtaining the geometric means of the ratios of Tx-Tf and C_6-NBD-SM fluorescence in individual recycling compartments from the double-labeled images described above. The ratios in the recycling compartment at the indicated chase times were averages (±SD) calculated from two separate experiments. Each data point in an experiment was normalized to the average ratio for the whole experiment. The average ratios were 0.911 ± 0.069 for experiment 1 and 1.6386 ± 0.198 for experiment 2.

To rule out the possibility that the similarity in the rates of sphingomyelin and Tf recycling is a fortuitous coincidence in TRVb-1 cells, we also measured the rates of exit of C_6-NBD-SM and Tx-Tf from the recycling compartment in a different CHO cell line, WTB111 cells (Robbins et al., 1984). These are ouabain resistant CHO cells, expressing the endogenous hamster Tf-R, and were derived from the same parental cell line from which TRVb-1 cells were obtained. They externalize Tf at a significantly faster rate ($t_{1/2}$ ~2.3 min; Johnson, L. S., J. F. Presley, K. W. Dunn, J. C. Park, and T. E. McGraw, manuscript submitted for publication) than TRVb-1 cells. The cells were labeled with C_6-NBD-SM and Tx-Tf for 30 min at 0°C, pulsed for 2 min at 37°C, stripped of surface bound lipid and Tf as described in Materials and Methods, and subsequently chased at 37°C for increasing lengths of time up to 7 min. Under these conditions, there was minimal hydrolysis of the internalized C_6-NBD-SM (<5% of the internalized sphingomyelin was converted to ceramide and no glucosylceramide was detected). The rates of exit of C_6-NBD-SM and Tx-Tf from the recycling compartment were 2.4 min^{-1} and 2.1 min^{-1}, respectively. Although the kinetics of traffic for both lipid and Tf in WTB111 cells are faster than that in TRVb-1 cells, the fluorescent patterns at the end of the pulse and chase are similar to those depicted in Fig. 3. The mean ratios of C_6-NBD-SM and Tx-Tf fluorescence in individual recycling compartments were also determined at each time point and found to be constant throughout the chase period (0.674 ± 0.07), confirming that C_6-NBD-SM and Tx-Tf exit the recycling compartment at the same rate.

Along with the results shown in Fig. 7, these data show that after leaving the sorting endosome C_6-NBD-SM and Tx-Tf, with indistinguishable kinetics, accumulate in the recycling compartment and exit this compartment before exiting the cell.

Discussion

C_6-NBD-SM as a Bulk Membrane Marker

A significant fraction of total cellular phospholipids (~70–90% of the total sphingomyelin and ~30–50 of phosphatidylcholine) is located at the plasma membrane in eukaryotic cells, and 50–80% of total membrane surface area is occupied by phospholipids (Koval and Pagano, 1991; Lange et al., 1989; van Meer, 1989). Sphingomyelin and phosphatidylcholine are asymmetrically located in the exoplasmic leaflet of the plasma membrane and have a very low rate of transbilayer flip-flop, at least at the plasma membrane (for review see Devaux, 1991), and exogenously introduced fluorescent analogs of phosphatidylcholine (C_6-NBD-PC) and sphingomyelin (C_6-NBD-SM) do not translocate to the cytoplasmic surface during the endocytic process (Koval and Pagano, 1989; Sleight and Pagano, 1984). Furthermore, the rate of internalization of C_6-NBD-SM measured in CHO cells (~1.5% internalized per minute; [Koval and Pagano, 1989] and unpublished observations) is comparable to bulk membrane endocytic rates (~1.6% of plasma membrane area internalized per minute) determined by stereological analyses and rates of bulk fluid phase endocytosis in BHK cells (Griffiths et al., 1989). We have found that the amount of endosome fluorescence increases linearly with the amount

of lipid incorporated at the plasma membrane. At present we do not know what proportion of C_6-NBD-SM is internalized via coated pits since some cell surface molecules such as glycolipids and glycolipid-binding proteins, ricin, cholera, and tetanus toxin, are internalized via noncoated pit mediated endocytosis in addition to clathrin-mediated endocytosis (for review see van Deurs et al., 1989). These two pathways appear to merge at the level of the peripherally distributed sorting endosomes (Raub et al., 1990*a*; Tran et al., 1987), and our data show that in TRVb-1 cells, as early as 2 min, greater than 80% of the total internalized C_6-NBD-SM fluorescence is colocalized with Tf. Cumulatively, these data show that C_6-NBD-SM is internalized via a constitutive 'bulk' process into the endocytic system and can be used as a marker for bulk membrane flow through the endocytic compartments.

Endocytic Fate of a Bulk Membrane Marker

The data presented in this report show that internalized C_6-NBD-SM and Tx-Tf are first visualized in sorting endosomes, colocalized with lysosomally directed ligands (e.g., α_2M and LDL). These compartments have been previously characterized in CHO cells as tubular vesicular organelles where Tf and α_2M (Yamashiro et al., 1984) and WGA (Raub et al., 1990*a*,*b*) are delivered soon after internalization. Unlike lysosomally directed ligands which accumulate in sorting endosomes for several minutes, Tx-Tf and C_6-NBD-SM simultaneously and rapidly come to a steady state in this compartment. C_6-NBD-SM and Tx-Tf then rapidly exit the sorting endosome ($t_{1/2}$s ~2.5 min) and accumulate in the recycling compartment with similar kinetics. The constancy in the ratios of Tx-Tf and C_6-NBD-SM fluorescence in sorting endosomes at different chase times confirmed that the two molecules leave the sorting endosome at the same rate. This rate is consistent with the previously observed rate of exit of Tf from sorting endosomes ($t_{1/2}$ <3 min), measured by determining the kinetics of loss of fusion accessibility of F-Tf to subsequently endocytosed anti-fluorescein antibody (Salzman and Maxfield, 1989). This rate also corresponds to the rate of sorting of Tf from LDL qualitatively determined in CHO cells ($t_{1/2}$ <3 min; Dunn et al., 1989) and to the rate of sorting of Tf and asialoglycoprotein measured in an hepatocyte cell line by Stoorvogel et al. ($t_{1/2}$ ~2 min; Stoorvogel et al., 1987).

The similarity of the ratio of lipid to Tf fluorescence in sorting endosomes with that measured in the recycling compartment shows that the same proportion of lipid and Tf that leaves the sorting endosomes arrives in the recycling endosomal compartment, arguing against any selectivity for transport of recycling receptors over bulk membrane. These data do not rule out the possibility that a fraction of both lipid and Tf may be directly recycled back to the cell surface from sorting endosomes. However, if this is so, the same fraction of both molecules must be diverted along this route.

Recycling Back to the Cell Surface Takes Place Via a Separate Recycling Endosomal Compartment

After exiting the sorting endosomes, en route to the cell surface, C_6-NBD-SM and Tx-Tf accumulate in the peri-centriolar recycling compartment, with identical kinetics. Intracellular accumulation of several membrane-associated molecules including C_6-NBD-PC, Tf-R, and the LDL receptor (McGraw et al., 1993) in the recycling compartment en route to the cell surface in different CHO cell lines indicates that this compartment is involved in the recycling of a majority of molecules back to the cell surface after they are sorted from lysosomally directed ligands. The difference in pH observed between the sorting endosomes (pH ~6.0) and recycling compartment (pH ~6.4) (Yamashiro et al., 1987, 1984; Presley, J. F., S. Mayor, K. W. Dunn, L. S. Johnson, T. E. McGraw, and F. R. Maxfield, manuscript submitted for publication), and the pulse-chase data presented here provide compelling evidence for a separate recycling compartment as a functional subdivision of early endosomes.

The rate of exit of C_6-NBD-SM and Tx-Tf from the recycling compartment ($t_{1/2}$ ~10 min) is indistinguishable from the rate of efflux of Tf and C_6-NBD-SM from whole cells. In experiments carried out in TRVb-1 cells, the half-time for the exit of Tf from TRVb-1 cells was ~10 min, identical to the rate obtained for C_6-NBD-SM exit in the same cells, determined by spectrophotometrically measuring the rate of appearance of lipid in the chase medium (Presley, J. F., S. Mayor, K. W. Dunn, L. S. Johnson, T. E. McGraw, and F. R. Maxfield, manuscript submitted for publication). In WTB cells where the rate of exit of Tf is different from the corresponding rate in TRVb-1 cells, C_6-NBD-SM and Tx-Tf also exit the recycling compartment in these cells at the same rate as the exit of Tf from the WTB cells. Thus, the rate limiting step in exit of C_6-NBD-SM and Tx-Tf from cells is exit from the recycling compartment.

The ratios of C_6-NBD-SM and Tx-Tf fluorescence in the recycling compartment during the chase period were essentially constant, confirming that the Tf and bulk membrane leave this compartment with identical kinetics, possibly in the same vesicles. An unambiguous confirmation of the route taken by these two molecules back to the cell surface was not possible because intermediate steps (presumably small vesicles) were not visualized. However, the identical kinetics of recycling of Tf and C_6-NBD-SM in the different cell lines strongly suggests that recycling does not require specific peptide signals.

Efficient Recycling Is a Default Pathway

The identical pathways of the bulk membrane marker, C_6-NBD-SM and Tf can be most easily understood if recycling of membrane components is a default pathway in the endocytic system. Data on several membrane molecules are consistent with this interpretation (for review see Courtoy, 1991; Steinman et al., 1983; van Deurs et al., 1989). The rates of externalization of a variety of receptors in alveolar macrophages were found to be independent of the nature of the receptors internalized (Ward et al., 1989). Mutant Tf receptors, differing in internalization rates due to cytoplasmic tail mutations or deletions also recycled efficiently, and exited the cell at the same rate as wild type receptors (Jing et al., 1990; McGraw and Maxfield, 1990; McGraw et al., 1991). Furthermore, other C_6-NBD-derivatized lipids, glucosylceramide (Kok et al., 1989), galactosylceramide, and PC (Sleight and Abanto, 1989; Sleight and Pagano, 1984; and this report) also enter the endocytic route, colocalized with transferrin, and are recycled.

Cumulatively, these observations show that bulk membrane along with membrane proteins are efficiently directed towards the recycling pathway, demonstrating that recycling of membrane components is a default pathway.

Geometric Basis for Sorting in the Endocytic System

While membrane components are efficiently recycled back to the cell surface, acid-released ligands (α_2M and LDL) and bulk fluid (e.g., HRP) are lysosomally directed, albeit with lower efficiencies (Adams et al., 1982; Besterman et al., 1982; Greenspan and St. Clair, 1984; Yamashiro et al., 1989). Retained acid-released ligands and fluid phase molecules are then delivered to the late endosomes and lysosomes at the same rate (Ward et al., 1989), via a maturation process (Dunn and Maxfield, 1992; Stoorvogel et al., 1991). The small amount of fluid phase (e.g., HRP) recycling has been shown to take place via a tubular-network of endosomes in the peri-centriolar region of HeLa and AtT20 cells (Tooze and Hollinshead, 1991), presumably similar to the recycling compartment described in CHO cells.

Sorting between recycling and lysosomally directed molecules in the endocytic system thus represents a 'bulk phase separation' and primarily reduces to sorting between membrane-associated molecules and fluid-phase molecules. Sorting endosomes have been characterized in BHK cells (early endosomes; Griffiths et al., 1989; Marsh et al., 1986) and CHO cells (Raub et al., 1990*a*; Yamashiro et al., 1984). They consist of a few narrow diameter (~50–60 nm) tubules attached to spherical vesicles ~250–500 nm in diameter. Estimates of the relative surface areas in the tubules of the sorting endosome vary from 50 to 80% while the majority (60–70%) of the volume is located in the spherical portion of the endosome (Griffiths et al., 1989; Marsh et al., 1986). Although the budding off of tubules and their direction towards the recycling pathway in a single step would not account for efficient recycling of membrane components (Linderman and Lauffenburger, 1988), this feature can be explained by an iterative fractionation process taking advantage of the geometry of sorting endosomes (Dunn et al. 1989). In this process, sorting would take place by the iterative formation and budding off of narrow-diameter tubules of greater surface area to volume ratio than the spherical vesicular body of the sorting endosome. The tubules would then be directed towards the recycling pathway. Dunn et al. (1989) have shown that sorting endosomes undergo multiple cycles of fusion and fission, consequently removing recycling components (Tf and Tf-R) and concomitantly accumulating lysosomally directed ligands (acid-released LDL). Given the observed geometric parameters of sorting endosomes, this iterative process would quickly result (within 20–30 cycles) in efficient removal of nearly all membrane components, while retaining most of the luminal content (Dunn et al., 1989). It is still possible that for certain receptors, the efficiency of sorting may be enhanced by selective recruitment into tubules (Geuze et al., 1987). However, our data indicate that this is not the case for Tf-R.

The model of 'default sorting' by an iterative fractionation process implies that only a minor fraction of the internalized membrane would be delivered to lysosomes. This is consistent with data from biochemical experiments where such measurements have been made: a minor fraction (<5%) of internalized C_6-NBD-SM was delivered to late endosomes/lysosomes (Koval and Pagano, 1990). The presence of lysosomal acid–sphingomyelinase in wild-type fibroblasts and CHO cells has prevented the detection of the small amount of lipid that is directed towards the lysosomal pathway (Koval and Pagano, 1990; and this report). However, in a mutant fibroblast cell line lacking the lysosomal acid–sphingomyelinase, Koval and Pagano (1990) have observed lysosomal delivery of small amounts of C_6-NBD-SM after relatively long pulse and chase times.

Exceptions to Default Recycling

An important implication of default recycling of membrane components is that specific retention signals would be required to redirect a significant fraction of any particular membrane component towards the lysosomal pathway. Aggregation, induced by multivalent binding of polyvalent antibodies, or multimeric ligands have been shown to reroute recycling molecules towards the lysosomally directed pathway (Mellman and Plutner, 1984; Weismann et al., 1986). Aggregated lipid domains such as those formed by N-labeled phosphatidylethanolamine are also routed to the lysosome (Kok et al., 1990). Thus, aggregation may be a general signal for lysosomal-targeting. Specific peptide sequences such as the cytoplasmic sequence found on lysosomal acid phosphatase may also redirect membrane molecules towards the lysosomal pathway (Braun et al., 1989; Peters et al., 1990). Studies with kinase-defective and kinase-active EGF receptors provide some evidence for ligand-induced signals involved in mediating the removal of membrane receptors from the recycling pathway (Felder et al., 1990; Honegger et al., 1990). When mutant and wild type EGF receptors were internalized, only the kinase-active receptors were delivered to lysosomes and were found in the membrane invaginations and internal vesicles of multivesicular endosomes while the kinase-defective receptors were efficiently recycled (Felder et al., 1990). This may be a general mechanism for retaining specific membrane-associated molecules in the sorting endosome, involving the formation of membrane invaginations and inward pinching off of vesicles into the lumen of the sorting endosome (Hopkins, 1992).

Conclusion

The data presented in this paper show that bulk membrane, although internalized at 10-fold slower rates than Tf-R, traffics through the same compartments and at identical rates as Tf-R. This demonstrates a default recycling pathway for membrane components via sorting endosomes and the recycling compartment en route to the cell surface. The rate of entry of different receptors or proteins into this pathway is dictated by the efficiency of entrapment in clathrin-coated pits at the plasma membrane. Unless specifically sorted (or filtered; Hopkins, 1992) towards the lysosome in sorting endosomes, membrane-associated molecules will recycle as bulk membrane. Luminal fluid including acid-released ligands will be mainly lysosomally directed by default (due to geometric considerations).

The model of sorting based on geometry and iterative fractionation places a primary role on the actual structure of the sorting endosome and predicts that control of structural de-

terminants of the sorting endosome (e.g., diameter and extent of tubulation) as well as its fusion and budding properties would have a profound influence on the rates and efficiencies of sorting of membrane components from luminal fluid phase. The molecular basis for controlling these properties are not well understood but proteins such as small GTPases, rab4 and rab5, may play a role in these functions (Bucci et al., 1992; van der Sluijs et al., 1992).

We would like to acknowledge Mike Hillmeyer and Jeff Myers for their sustained help with image processing routines and computer related matters, and Ira Tabas for a generous gift of LDL. We would like to thank Ken Dunn and G. van Meer for useful suggestions, and K. Dunn, Richik Ghosh, Tim McGraw, and Anant Menon for critically reading the manuscript. S. Mayor would like to thank S. J. Gould for inspiration.

This work was supported by a grant from the Helen Hay Whitney Foundation to S. Mayor and National Institutes of Health grants DK27083 to F. R. Maxfield and CA09503-08 to J. F. Presley. The costs of publication of this article were defrayed in part by the payment of page charges. This article must therefore be hereby marked advertisement in accordance with 18 USC Section 1734 solely to indicate this fact.

Received for publication 25 January 1993 and in revised form 19 March 1993.

References

Adams, C. J., K. M. Maurey, and B. Storrie. 1982. Exocytosis of pinocytic contents by chinese hamster ovary cells. *J. Cell Biol.* 93:632–637.

Besterman, J. M., J. A. Airhart, R. C. Woodworth, and R. B. Low. 1982. Exocytosis of pinocytosed fluid in cultured cells: kinetic evidence for rapid turnover and compartmentation. *J. Cell Biol.* 91:716–727.

Braun, M., A. Waheed, and K. von Figura. 1989. Lysosomal acid phosphatase is transported to lysosomes via the cell surface. *EMBO (Eur. Mol. Biol. Organ.) J.* 8:3633–3640.

Bucci, C., R. G. Parton, I. H. Mather, H. Stunnenberg, K. Simons, B. Hoflack, and M. Zerial. 1992. The small GTPase rab5 functions as a regulatory factor in the early endocytic pathway. *Cell.* 70:715–728.

Courtoy, P. J. 1991. Dissection of endosomes. *In* Intracellular Trafficking of Proteins. C. J. Steer and J. A. Hanover, editors. Cambridge University Press, Cambridge. 157–182.

Devaux, P. F. 1991. Static and dynamic lipid asymmetry in cell membranes. *Biochemistry.* 30:1163–1172.

Dunn, K. W., and F. R. Maxfield. 1992. Delivery of ligands from sorting endosomes to late endosomes occurs by maturation of sorting endosomes. *J. Cell Biol.* 117:301–310.

Dunn, K. W., T. E. McGraw, and F. R. Maxfield. 1989. Iterative fractionation of recycling receptors from lysosomally destined ligands in an early sorting endosome. *J. Cell Biol.* 109:3303–3314.

Felder, S., K. Miller, G. Moehren, A. Ullrich, J. Schlessinger, and C. Hopkins. 1990. Kinase activity controls sorting of the epidermal growth factor receptor within the multivesicular body. *Cell.* 61:623–634.

Geuze, H. J., J. W. Slot, and A. L. Schwartz. 1987. Membranes of sorting organelles display lateral heterogeneity in receptor distribution. *J. Cell Biol.* 104:1715–1723.

Geuze, H. J., J. W. Slot, G. J. A. M. Strous, H. F. Lodish, and A. L. Schwartz. 1983. Intracellular site of asialoglycoprotein receptor-ligand uncoupling: double-label immunoelectron microscopy during receptor-mediated endocytosis. *Cell.* 32:277–287.

Goldstein, J. L., M. S. Brown, R. G. W. Anderson, D. W. Russell, and W. J. Schneider. 1985. Receptor mediated endocytosis: concepts emerging from the LDL receptor system. *Annu. Rev. Cell Biol.* 1:1–39.

Greenspan, P., and R. W. St. Clair. 1984. Retroendocytosis of low density lipoprotein: effect of lysosomal inhibitors on the release of undegraded 125-low density lipoprotein of altered composition from skin fibroblasts in culture. *J. Biol. Chem.* 259:1703–1713.

Griffiths, G., R. Back, and M. Marsh. 1989. A quantitative analysis of the endocytic pathway in baby hamster kidney cells. *J. Cell Biol.* 109:2703–2720.

Gruenberg, J., G Griffiths, and K. E. Howell. 1989. Characterization of the early endosome and putative endocytic carrier vesicles in vivo and with an assay of vesicle fusion in vitro. *J. Cell Biol.* 108:1301–1316.

Hirschfeld, T. 1976. Quantum efficiency independence of the time integrated emission from a fluorescent molecule. *Applied Optics.* 15:3135–3139.

Honegger, A. M., A. Schmidt, A. Ullrich, and J. Schlessinger. 1990. Separate endocytic pathways of kinase-defective and -active EGF receptor mutants expressed in same cells. *J. Cell Biol.* 110:1541–1548.

Hopkins, C. R. 1992. Selective membrane protein trafficking: vectorial flow and filter. *Trends Biochem. Sci.* 17:27–32.

Jing, S., T. Spencer, K. Miller, C. Hopkins, and I. S. Trowbridge. 1990. Role of the human transferrin receptor cytoplasmic domain in endocytosis: localization of a specific signal sequence for internalization. *J. Cell Biol.* 110: 283–294.

Jovin, T. M., and D. J. Arndt-Jovin. 1989. FRET microscopy: digital imaging of fluorescence resonance energy transfer. Application in Cell Biology. *In* Cell Structure and Function by Microspectrofluorometry. E. Kohen and J. G. Hirschberg, editors. Academic Press, San Diego. 99–117.

Kishimoto, Y. 1975. A facile synthesis of ceramides. *Chem. Phys. Lipids.* 15:33–36.

Kok, J. W., S. Eskelinen, K. Hoekstra, and D. Hoekstra. 1989. Salvage of glucosylceramide by recycling after internalization along the pathway of receptor mediated endocytosis. *Proc. Natl. Acad. Sci. USA.* 86:9896–9900.

Kok, J. W., M. ter Beest, G. Scherphof, and D. Hoekstra. 1990. A non-exchangeable fluorescent phospholipid analog as a membrane traffic marker of the endocytic pathway. *Eur. J. Cell Biol.* 53:173–184.

Koval, M., and R. E. Pagano. 1989. Lipid recycling between the plasma membrane and intracellular compartments: transport and metabolism of fluorescent sphingomyelin analogues in cultured fibroblasts. *J. Cell Biol.* 108: 2169–2181.

Koval, M., and R. E. Pagano. 1990. Sorting of an internalized plasma membrane lipid between recycling and degradative pathways in normal and Niemann-Pick, type A fibroblasts. *J. Cell Biol.* 111:429–442.

Koval, M., and R. E. Pagano. 1991. Intracellular transport and metabolism of sphingomyelin. *Biochim. Biophys. Acta.* 1082:113–125.

Kremer, J. M. H., M. W. J. v. d. Esker, C. Pathmamanoharan, and P. H. Wiersema. 1977. Vesicles of variable diameter prepared by a modified injection method. *Biochemistry.* 16:3932–3935.

Labarca, C., and K. Paigen. 1980. A rapid, simple, and sensitive DNA assay procedure. *Anal. Biochem.* 102:344–352.

Lange, Y., M. H. Swaisgood, B. V. Ramos, and T. L. Steck. 1989. Plasma membranes contain half the phospholipid and 90% of the cholesterol and sphingomyelin in cultured fibroblasts. *J. Biol. Chem.* 264:3786–3793.

Linderman, J. J., and D. A. Lauffenburger. 1988. Analysis of intracellular receptor/ligand sorting in endosomes. *J. Theor. Biol.* 132:203–245.

Marsh, M., G. Griffiths, G. E. Dean, I. Mellman, and A. Helenius. 1986. Three-dimensional structure of endosomes in BHK-21 cells. *Proc. Natl. Acad. Sci. USA.* 83:2899–2903.

Maxfield, F. R., and K. W. Dunn. 1990. Studies of endocytosis using image intensification fluorescence microscopy and digital image analysis. *In* Optical Microscopy for Biology. B. Herman and K. Jackson, editors. Wiley-Liss, New York. 357–371.

Maxfield, F. R., and D. J. Yamashiro. 1991. Acidification of organelles and the intracellular sorting of proteins during endocytosis. *In* Intracellular Trafficking of Proteins. C. J. Steer and J. A. Hanover, editors. Cambridge University Press, Cambridge. 157–182.

Mayor, S., and F. R. Maxfield. 1993. Direct comparison of the endocytic routes of fluorescently-labeled lipids and transferrin. *In* Molecular Mechanisms of Membrane Traffic. NATO ASI Series H, Vol. 74. D. J. Morre, K. M. Howell, and J. J. M. Bergeron, editors. Springer-Verlag, Berlin. 269–272.

McGraw, T. E., and F. R. Maxfield. 1990. Human transferrin receptor internalization is partially dependent upon an aromatic amino acid on the cytoplasmic domain. *Cell Regulation.* 1:369–377.

McGraw, T. E., L. Greenfield, and F. R. Maxfield. 1987. Functional expression of human transferrin receptor cDNA in Chinese hamster ovary cells deficient in endogenous transferrin receptor. *J. Cell Biol.* 105:207–214.

McGraw, T. E., K. W. Dunn, and F. R. Maxfield. 1993. Isolation of a temperature-sensitive variant CHO cell line with a morphologically altered endocytic recycling compartment. *J. Cell Physiol.* In press.

McGraw, T. E., B. Pytowski, J. Artz, and C. Ferrone. 1991. Mutagenesis of human transferrin receptor: two cytoplasmic phenylalanines are required for efficient internalization and a second-site mutation is capable of reverting an internalization defective phenotype. *J. Cell Biol.* 112:853–861.

Mellman, I., and H. Plutner. 1984. Internalization and degradation of macrophage Fc receptors bound to polyvalent immune complexes. *J. Cell Biol.* 98:1170–1177.

Mellman, I., R. Fuchs, and A. Helenius. 1986. Acidification of the endocytic and exocytic pathways. *Annu. Rev. Biochem.* 55:663–700.

Nichols, J. W., and R. E. Pagano. 1981. Kinetics of soluble lipid monomer diffusion between vesicles. *Biochemistry.* 20:2783–2789.

Peters, C., M. Braun, B. Weber, M. Wendland, B. Schmidt, R. Pohlmann, A. Waheed, and K. von Figura. 1990. Targeting of a lysosomal membrane protein: a tyrosine-containing endocytosis signal in the cytoplasmic tail of lysosomal acid phosphatase is necessary and sufficient for targeting to lysosomes. *EMBO (Eur. Mol. Biol. Organ) J.* 9:3633–3640.

Pitas, R. E., T. L. Innerarity, J. N. Weinstein, and R. W. Mahley. 1981. Acetoacetylated lipoproteins used to distinguish fibroblasts from macrophages in vitro by fluorescence microscopy. *Arteriosclerosis.* 1:177–185.

Raub, T. J., M. J. Koroly, and R. M. Roberts. 1990*a*. Endocytosis of wheat germ agglutinin binding sites from the cell surface into a tubular endosomal network. *J. Cell Physiol.* 143:1–12.

Raub, T. J., M. J. Koroly, and R. M. Roberts. 1990*b*. Rapid endocytosis and recycling of wheat germ agglutinin binding sites on CHO cells: evidence for two compartments in a nondegradative pathway. *J. Cell Physiol.* 144:52–61.

Robbins, A. R., C. Oliver, J. L. Bateman, S. S. Krag, C. J. Galloway, and

I. Mellman. 1984. A single mutation in Chinese hamster ovary cells impairs both Golgi and endosome functions. *J. Cell Biol.* 99:1296–1308.
Rome, L. 1985. Curling receptors. *Trends Biochem. Sci.* 10:151.
Salzman, N. H., and F. R. Maxfield. 1989. Fusion accessibility of endocytic compartments along the recycling and lysosomal endocytic pathways in intact cells. *J. Cell Biol.* 109:2097–2104.
Sleight, R. G., and R. E. Pagano. 1984. Transport of a fluorescent phosphatidylcholine analog from the plasma membrane to the Golgi apparatus. *J. Cell Biol.* 99:742–751.
Sleight, R. G., and M. N. Abanto. 1989. Differences in the intracellular transport of a fluorescent phosphatidylcholine analog in established cell lines. *J. Cell Sci.* 93:363–374.
Steinman, R. M., I. S. Mellman, W. A. Muller, and Z. A. Cohn. 1983. Endocytosis and recycling of plasma membrane. *J. Cell Biol.* 96:1–27.
Stoorvogel, W., H. J. Geuze, and G. J. Strous. 1987. Sorting of endocytosed transferrin and asialoglycoprotein occurs immediately after internalization in HepG2 cells. *J. Cell Biol.* 104:1261–1268.
Stoorvogel, W., G. J. Strous, H. J. Geuze, V. Oorschot, and A. L. Schwartz. 1991. Late endosomes derive from early endosomes by maturation. *Cell.* 65:417–427.
Tooze, J., and M. Hollinshead. 1991. Tubular early endosomal networks in AtT20 and other cells. *J. Cell Biol.* 115:635–653.
Tran, D., J.-L. Carpentier, F. Sawano, P. Gorden, and L. Orci. 1987. Ligands internalised through coated and noncoated invaginations follow a common intracellular pathway. *Proc. Natl. Acad. Sci. USA.* 84:7957–7961.
van der Sluijs, P., M. Hull, P. Webster, P. Male, B. Goud, and I. Mellman. 1992. The small GTP-binding protein rab4 controls an early sorting event on the endocytic pathway. *Cell.* 70:729–740.
van Deurs, B., O. W. Petersen, S. Olsnes, and K. Sandvig. 1989. The ways of endocytosis. *Int. Rev. Cytol.* 117:131–177.
van Meer, G. 1989. Lipid transport in animal cells. *Annu. Rev. Cell Biol.* 5:247–275.
van Meer, G., E. H. K. Stelzer, R. W. Wijnaendts-van-Resandt, and K. Simons. 1987. Sorting of sphingolipids in epithelial (Madin-Darby canine kidney) cells. *J. Cell Biol.* 105:1623–1635.
Ward, D. M., R. Ajioka, and J. Kaplan. 1989. Cohort movement of different ligands and receptors in intracellular endocytic pathway of alveolar macrophages. *J. Biol. Chem.* 264:8164–8170.
Weismann, A. M., R. D. Klausner, K. Rao, and J. B. Harford. 1986. Exposure of K562 cells to anti-receptor monoclonal antibody OKT9 results in rapid redistribution and enhanced degradation of the transferrin receptor. *J. Cell Biol.* 102:951–958.
Yamashiro, D. J., and F. R. Maxfield. 1987. Acidification of morphologically distinct endosomes in mutant and wild-type Chinese hamster ovary cells. *J. Cell Biol.* 105:2723–2733.
Yamashiro, D. J., B. Tycko, S. R. Fluss, and F. R. Maxfield. 1984. Segregation of transferrin to a mildly acidic (pH 6.5) para-Golgi compartment in the recycling pathway. *Cell.* 37:389–800.
Yamashiro, D. J., L. A. Borden, and F. R. Maxfield. 1989. Kinetics of α_2-macroglobulin endocytosis and degradation in mutant and wild-type Chinese hamster ovary cells. *J. Cell Physiol.* 139:377–382.